International Journal of Pharmaceutics 649 (2024) 123639

Contents lists available at ScienceDirect

International Journal of Pharmaceutics

journal homepage: www.elsevier.com/locate/ijpharm

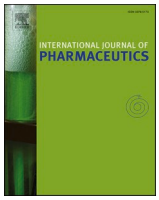

3D-printed prednisolone phosphate suppositories with tunable dose and rapid release for the treatment of inflammatory bowel disease

L.I. Kocabas [a,*], S. Ayyoubi [a], M. Tajqurishi [a], J. Quodbach [a], T. Vermonden [a], R.J. Kok [a]

[a] Division of Pharmaceutics, Department of Pharmaceutical Sciences, Utrecht Institute for Pharmaceutical Sciences (UIPS), Utrecht University, Utrecht 3584 CG, the Netherlands

ARTICLE INFO

Keywords:
Fused deposition modeling
Hot-melt extrusion
Rectal administration
Infill density
Personalized medicine

ABSTRACT

Established medicines are often not tailored to the needs of the pediatric population, causing difficulties with administration or dosing. Three-dimensional (3D) printing technology allows novel approaches for compounding of personalized medicine, as is exemplified in this study for the automated compounding of rectal preparations for children. We investigated the material requirements to print prednisolone phosphate-loaded suppositories with tunable dose and rapid drug release for the treatment of inflammatory bowel diseases. Three formulations containing 4 % w/w prednisolone sodium phosphate (PSP) and different amounts of hydroxypropyl cellulose (HPC) and mannitol as excipients were printed as suppositories with a fused deposition modeling (FDM) 3D-printer. Dissolution studies showed that the PSP release rate was increased when higher weight fractions of mannitol were added as a pore former, with 90 % drug release within 30 min for mannitol 48 % w/w. We further printed suppositories with 48 % mannitol with different infill densities and dimensions to tune the dose. Our findings demonstrated that 3D-printed suppositories with PSP doses ranging from 6 to 30 mg could be compounded without notably affecting the dissolution kinetics, ensuring equivalent therapeutic efficacies for different doses.

1. Introduction

Existing dosage forms are frequently not suitable for children. Young infants experience difficulties with swallowing oral solid dosage forms (Bowles et al., 2010). Furthermore, children often need doses tailored to their body weight. One approach to overcome these problems is the manufacturing or compounding of oral liquid medication that can be dispensed by volume. However, oral liquid medication is often not readily accepted due to taste aversion (Karavasili et al., 2021). Moreover, stability of liquid preparations is generally low and studies have demonstrated poor dosing accuracy of liquid preparations (Sobhani et al., 2008; Elliott et al., 2014; Arenas-López et al., 2017).

Alternative administration routes like the rectal route instead of oral drug intake can therefore be advantageous for pediatric medicines. Other advantages of the rectal route include bypassing of the first-pass effect and the possibility of administering medication in case of nausea and vomiting (Rathi et al., 2022). Consequently, suppositories provide a suitable alternative administration route for multiple indications. However, available rectal formulations are often fixed-dose preparations and dose flexibility can be a problem (Jannin et al., 2014).

Suppositories are a suitable dosage form for the treatment of inflammatory bowel diseases (IBD), such as ulcerative colitis (UC) and Crohn's disease. UC and Crohn's disease are chronic inflammatory disorders that affect the gastrointestinal tract. The incidence of IBD is increasing, especially in the pediatric population (Rosen et al., 2015; Kelsen et al., 2019). Pharmacotherapy of IBD is complex and relies on controlling symptoms through the use of a variety of drugs. In case of an exacerbation, oral corticosteroids, such as prednisolone, can be administered to patients for several weeks and tapered (i.e., the incremental and decremental change in dose at the beginning and end of pharmacotherapy) once remission is reached (Jeong et al., 2019; van Rheenen et al., 2021). A *meta*-analysis suggested that rectal corticosteroids can be an alternative treatment for UC in case of allergy or poor response to aminosalicylates (Marshall and Irvine, 1997). However, IBD treatment

Abbreviations: 3D, three-dimensional; PSP, prednisolone sodium phosphate; HPC, hydroxypropyl cellulose; IBD, inflammatory bowel disease; UC, ulcerative colitis; FDM, fused deposition modeling; CAD, computer-aided design; HME, hot-melt extrusion; TGA, thermogravimetric analysis; DSC, differential scanning calorimetry; PXRD, powder X-ray diffraction, SEM, scanning electron microscopy; UPLC, ultra-performance liquid chromatography.

* Corresponding author.
E-mail address: l.i.kocabas@uu.nl (L.I. Kocabas).

https://doi.org/10.1016/j.ijpharm.2023.123639
Received 15 September 2023; Received in revised form 22 November 2023; Accepted 23 November 2023
Available online 30 November 2023

protocols on corticosteroids vary in recommended dosing for pediatric patients between countries and professionals and no general guidelines exist (van Rheenen et al., 2021). Currently, no automated manufacturing technologies for individualized suppositories exist.

Novel technologies such as three-dimensional (3D) printing can be used to personalize the dosages of many medicines. 3D-printing is a technique with countless applications (Trenfield et al., 2018). Healthcare is just one of the many fields in which 3D-printing technology has emerged in recent years. Besides the production of medical devices, promising advances have been made in the development of pharmaceuticals and in shaping drug delivery with 3D-printing (Fan et al., 2020).

Fused deposition modeling (FDM) is a 3D-printing technology that is particularly promising in the pharmaceutical field due to its versatility, simplicity, and low production costs. A drug-loaded filament is mechanically pushed into a print head that is heated above the glass transition temperature (T_g) of the filament's material. The softened material is extruded through a nozzle and deposited layer by layer on a printing bed. Thus, a shape that is predetermined by a digital 3D-model designed in computer-aided design (CAD) software is printed (Cailleaux et al., 2021). One advantage of FDM is that the model can be printed in different sizes and with different infill patterns and infill densities to modify the dose per unit or dissolution kinetics (Goyanes et al., 2017).

The filament required for FDM is produced using hot-melt extrusion (HME) (Korte and Quodbach, 2018a; Ponsar et al., 2020; Dumpa et al., 2021). HME is a processing technology established for the manufacturing of numerous materials in various shapes that found its way into the pharmaceutical industry over the last decades (Patil et al., 2016; Simões et al., 2021). In HME for pharmaceutical purposes, a powder mixture, containing one or more drugs, polymers, and other potential excipients (e.g., plasticizers), is placed into a gravimetric or volumetric feeder. The mixture is fed into the extruder and pushed through a barrel by one or more rotating screws, heated above the T_g of the polymer(s), and forced out of a die in the shape of a filament.

A 3D-printed rectal prednisolone preparation with dose flexibility that can be adjusted to individual patient characteristics (such as body weight) and tapering schedules can fulfill an unmet need in the treatment of children with IBD. 3D-printed prednisolone preparations have been printed and investigated before (Skowyra et al., 2015; Sadia et al., 2016; Robles-Martinez et al., 2019; Sjöholm et al., 2020). However, these preparations were not intended for rectal administration. Previous studies have printed suppositories using FDM before, but those were primarily empty suppository shells that could be loaded with a drug (Tagami et al., 2019; Tagami et al., 2020; Persaud et al., 2020). In another study, FDM was used to print molds for rectal and vaginal suppositories (Krezić et al., 2019). Until now, only semi-solid extrusion (SSE) has been used to print drug-loaded suppositories that contained drugs like tacrolimus, lidocaine, a combination of budesonide and tofacitinib, and infliximab (Seoane-Viaño et al., 2021; Chatzitaki et al., 2021, Awad et al., 2023a, Awad et al., 2023b). We now propose FDM for printing prednisolone phosphate-loaded suppositories.

The use of polymers suitable for FDM often results in dosage forms with slow release (Fanous et al., 2020). 3D-printed prednisolone tablets, in which polyvinyl alcohol (PVA) was used as the polymer, showed extended release profiles, releasing 80 % of the drug after 12 to 18 h (Skowyra et al., 2015). The aforementioned tacrolimus suppositories released 80 % of the drug in 120 min (Seoane-Viaño et al., 2021). This can be advantageous in certain situations, since extended release may improve the bioavailability of some drugs (Purohit et al., 2018; Choi et al., 1998; Ryu et al., 1999; Tenci et al., 2019). However, recent literature presents a shift to FDM prints with rapid release. For rectal treatments, rapid release would ensure drug absorption before expulsion of the formulation. The release rate can be increased by using formulations with immediate release, containing for example Eudragit E (a copolymer based on dimethylaminoethyl methacrylate, butyl methacrylate, and methyl methacrylate). However, these formulations often have low T_g values that can cause 3D-printed structures to collapse or deform (Sadia et al., 2016). A new approach to increase the release rate of FDM printed preparations is therefore needed.

In this study, we aim to investigate the material requirements to successfully 3D-print prednisolone phosphate-loaded suppositories with tunable dose and rapid drug release for pediatric use. A method to easily vary the dose by changing parameters, such as the infill density and size of each suppository, would prove useful for the weight-dependent dosing and tapering of prednisolone for infants with IBD. Furthermore, reducing the size of suppositories would likely improve patient acceptance. Changing these parameters should not affect the desired dissolution and pharmacokinetics of the drug and the preparation should have a high drug release rate to ensure absorption through the rectal route.

2. Materials and methods

2.1. Chemicals

Prednisolone sodium phosphate (PSP) was purchased from Fagron (Rotterdam, The Netherlands). Prednisolone was purchased from Spruyt Hillen (IJsselstein, The Netherlands). Klucel EF hydroxypropyl cellulose (HPC) with an average molecular weight of 80,000 Da and PEARLITOL 200 SD (mannitol) were kindly donated by Barentz (Hoofddorp, The Netherlands).

2.2. 3D-printing of suppositories

2.2.1. Hot-melt extrusion

For the preparation of filaments, a Felfil Evo (Turin, Italy) single-screw extruder was utilized. First, powder mixtures consisting of various ratios of PSP, HPC, and mannitol (Table 1) were mixed in a WAB Group TURBULA mixer (Muttenz, Switzerland) for five minutes to ensure homogeneity. Each batch mixed consisted of 50 g of material. The mixtures were added to the hopper of the extruder and processed through a 2.85 mm nozzle at 130 °C and 4 RPM. For a random 140 cm piece of filament with 48 % mannitol, the diameter was measured every 10 cm using an Antylia Scientific Fowler Ultra-Cal V caliper (Vernon Hills, USA) to investigate diameter variation.

2.2.2. 3D-design

The suppository shape was designed in Autodesk Inventor (San Rafael, USA). The shape and standard dimensions were based on 1.15 ml suppository molds for infants with a height of 26 mm unless mentioned otherwise (Table 1). The design was then exported as a stereolithography (.stl) file format and imported into Ultimaker's slicer application Cura (Utrecht, The Netherlands). The following printing parameters were selected: a layer height of 0.1 mm with 12 closed bottom layers and 12 closed top layers, a wall line count of 2, and a grid

Table 1
Formulations and characteristics of 3D-printed suppositories.

Suppository	Formulation	Infill density (%)	Height (mm)
A	4 % PSP, 96 % HPC	20	26
B	4 % PSP, 23 % mannitol, 73 % HPC	20	26
C	4 % PSP, 48 % mannitol, 48 % HPC	20	26
D	4 % PSP, 48 % mannitol, 48 % HPC	50	26
E	4 % PSP, 48 % mannitol, 48 % HPC	80	26
F	4 % PSP, 48 % mannitol, 48 % HPC	20	21
G	4 % PSP, 48 % mannitol, 48 % HPC	20	16

infill pattern. The standard infill density was set to 20 % unless mentioned otherwise for dose-tuning purposes (Table 1). When the height of the suppositories was changed, other dimensions were scaled uniformly.

2.2.3. Fused deposition modeling 3D-printing

For the printing of the suppositories, filaments were fed into an Ultimaker S3 3D-printer (Utrecht, The Netherlands), equipped with a 0.4 mm nozzle. Suppositories A–G were printed in triplicate at a temperature of 150 °C on a build plate with a temperature of 60 °C. Printed suppositories were weighed individually with an A&D Company Galaxy HR-250AZ analytical balance (Tokyo, Japan), labeled, and stored in a refrigerator in plastic containers. Extra suppositories were printed if needed for additional analyses.

2.3. Analysis of materials and products

2.3.1. Thermal analysis

Differential scanning calorimetry (DSC) analysis was performed to further determine the thermal properties of the raw and processed materials. A TA Instruments Discovery DSC (Hertfordshire, UK) was loaded with samples of 4–10 mg using aluminum (Tzero) pans and unpierced aluminum (Tzero) lids and heated from 25 °C to 100 °C to remove water, cooled down, and heated again to 10 °C below the degradation temperature of the sample (as determined by TGA analysis, see Fig. S1) at a heating rate of 3 °C/min and a 1 °C/min modulation. TA Instruments TRIOS was used for the analysis of the collected data.

2.3.2. Powder X-ray diffraction

Powder X-ray diffraction (PXRD) patterns were recorded on a Bruker D2 Phaser (Billerica, USA) with a cobalt anode to investigate the physical state of the drug and excipients in the formulations. The wavelength was 0.179 nm and the applied voltage and current were 30 kV and 10 mA, respectively. Raw materials, the physical powder mixture, a ground filament, and a ground suppository were placed on a circular rotating sample holder and scanned in the 2θ ranges of 5° to 85° (step size 0.05° per second).

2.3.3. Scanning electron microscopy

Scanning electron microscopy (SEM) images of filaments and suppositories were obtained using a Thermo Fisher Scientific Phenom Pro/ProX G6 Desktop SEM (Waltham, USA) at 10 kV. Samples were prepared by breaking off pieces of the filaments and suppositories and placing them on carbon tape. Samples were analyzed without additional platinum coating.

2.4. In vitro drug release

2.4.1. Dissolution tests and drug content

Dissolution studies were performed in triplicate to obtain *in vitro* drug release profiles of the 3D-printed suppositories. These studies were conducted with a paddle apparatus and dissolution vessels containing 250 ml of water at a temperature of 37 °C and stirred at 100 RPM. A sample of 200 µl was collected at each of the following time points: 5, 10, 15, 20, 25, 30, 45, 60, 90, and 120 min. The samples were stored at room temperature until analysis on the same day. If the dissolution was not complete at 120 min, one extra sample was collected after complete dissolution to determine the total drug content. Subsequently, each sample was analyzed with ultra-performance liquid chromatography (UPLC) using the method described in section 2.4.2. The same method was used to determine the drug contents of separate batches of filaments after dissolution in 250 ml water at 37 °C.

2.4.2. Ultra-performance liquid chromatography

Samples collected as described in section 2.4.1 were analyzed with a Waters Acquity UPLC (Milford, US) coupled with a UV detector (Waters Acquity TUV), operated at a wavelength of 254 nm. Of each collected sample of 200 µl, 7.5 µl was injected once without prior treatment and separated on a Waters Acquity Premier BEH C18 column (1.7 µm, 2.1 mm x 50 mm) using a mobile phase consisting of water-acetonitrile (75:25 v/v) adjusted to pH 2.0 with phosphoric acid (85 wt% in water). Because of partial hydrolysis of the phosphate ester during extrusion and printing, the amounts of PSP and prednisolone base released were determined using separate calibration methods for both PSP and prednisolone base, and then combined to calculate the total drug release of the suppositories upon complete dissolution. The same method was used to determine the total drug content of filaments.

3. Results and discussion

3.1. Overview of the study

We investigated the material requirements to successfully print prednisolone phosphate-loaded suppositories with tunable dose and rapid drug release. Fig. 1 shows a schematic overview of this study.

3.2. Thermal and morphological studies of raw materials

Fig. 2 shows the physico-chemical characterization of the raw materials. For PSP, desorption of water is visible starting at around 80 °C (Fig. 2a). PSP is a crystalline compound. However, the DSC thermogram did not show a melting peak of PSP below 250 °C due to its stable crystal lattice. This is consistent with previous literature where PSP shows no melting peak but only an endothermic peak at higher temperatures than measured in our study (Berthold et al., 1996). As expected, no peak was observed for the amorphous polymer HPC. Mannitol showed an endothermic peak at 166 °C, corresponding to the melting point of mannitol in literature (Kim et al., 2023). The PXRD results confirmed the crystalline nature of PSP and mannitol and the amorphous nature of HPC (Fig. 2b).

To prevent amorphization and recrystallization of the compounds that could potentially cause stability issues, extrusion and printing were performed below temperatures at which thermal events occur (i.e., 166 °C). On the other hand, a temperature high enough to allow plastic deformation of HPC is needed, i.e., above the T_g of the grade used in our experiments. The manufacturer mentions a dual T_g at 0 °C and 120 °C for HPC (Ashland Inc., 2017). Our measurements did not show the reported T_g's of HPC, even when heated from a starting temperature of –30 °C. The processing temperatures (130 °C for HME and 150 °C for 3D-printing) were therefore based on experimental results, as discussed in section 3.3. TGA showed that no decomposition of materials occurred at these processing temperatures (Fig. S1).

3.3. Prednisolone phosphate-loaded filaments and suppositories

3.3.1. Hot-melt extrusion of filaments

After the characterization of the raw materials, three different formulations with increasing mannitol contents were extruded. Mannitol was added as a pore-forming excipient to increase the drug release rate (Jaipal et al., 2015). The HME parameters were experimentally determined to be 130 °C and 4 RPM by extruding at different parameters (120–150 °C and 1–9 RPM) and assessing the filaments visually. Upon manual inspection, filaments containing mannitol were more brittle compared to filaments without mannitol but showed appropriate flexibility to be fed to the FDM printer.

In this study, an entry-level single-screw hot-melt extruder was used. The average diameter of a 140 cm piece of filament containing 48 % mannitol was 2.56 ± 0.07 mm (n = 15, Table S1). Thus, despite the low costs of our extruder, we were able to achieve a good filament diameter consistency. The addition of mannitol seemed to improve the consistency of filament diameter, possibly by improving the flowability of the material (see section 3.3.2.). Furthermore, single-screw extruders are

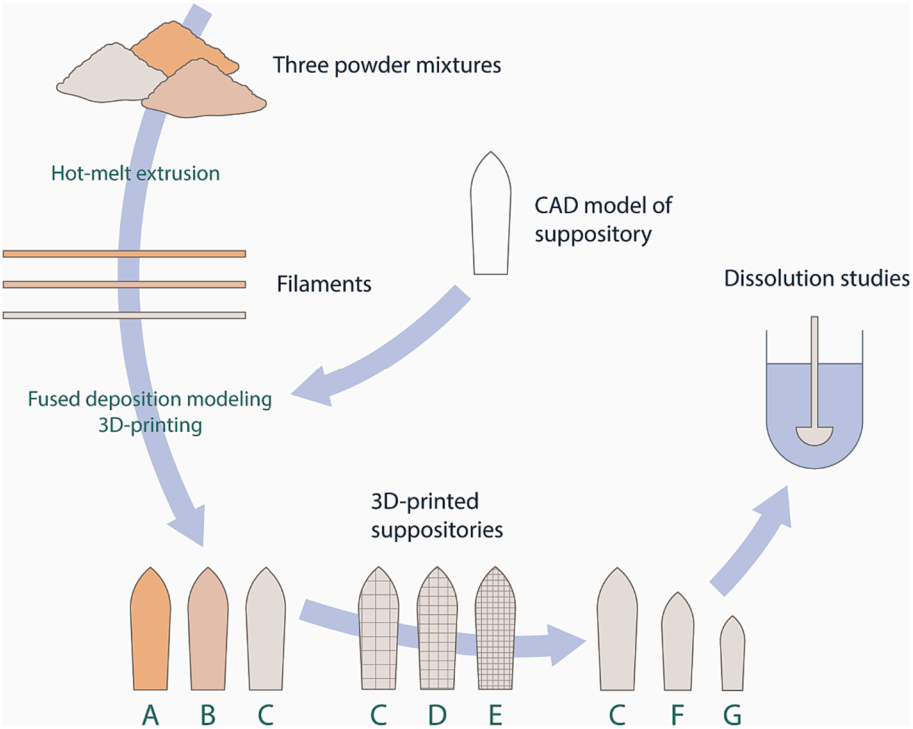

Fig. 1. Schematic overview of the study. Three powder formulations with 4% w/w prednisolone sodium phosphate and different concentrations of hydroxypropyl cellulose and mannitol were extruded and 3D-printed as suppositories (A, B, and C). The effect of mannitol concentration on drug release rate was investigated with dissolution studies. The formulation of the suppository with the highest release rate (C) was then used to print suppositories with different infill densities (D and E) and dimensions (F and G). Drug release rates of these suppositories were then compared to the release rate of suppository C to investigate the tunability of the drug loading.

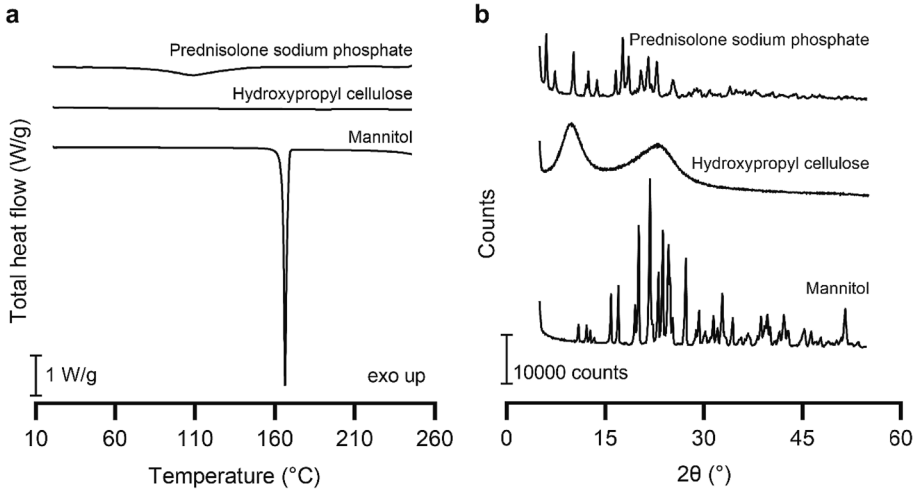

Fig. 2. Physical-chemical characterization of raw materials. a) Differential scanning calorimetry thermograms of drug and excipients. b) Powder X-ray diffraction of drug and excipients.

operating filled ensuring lower diameter variation. Filaments produced with twin-screw extruders show higher fluctuations compared to commercial filaments manufactured with single-screw extruders (Ponsar et al., 2020). Although our filaments did not reach the targeted diameter of 2.85 mm (the nozzle diameter used during extrusion), the good variation resulted in relative mass variations of < 10 % for all suppositories, which seems acceptable for PSP suppositories.

Table 2 and Table S2 show the drug contents of six randomly cut pieces of filament from two batches, demonstrating homogeneous distribution of the drug in filaments from the same batch but not in filaments from different batches. Only the batch with the desired drug release rate (i.e., 48 % mannitol) was analyzed. Variation between batches is possibly caused by pure drug material remaining in the hopper or the mixing container due to demixing or static charging since no drug degradation occurred (see section 3.3.2) and homogeneity within batches was high.

3.3.2. *Fused deposition modeling 3D-printing of suppositories*

After analysis of the filaments, new filaments were extruded and used to 3D-print different suppositories at 150 °C. Each type of suppository was printed in triplicate and individually weighed (Table 3 and Table S3). When corrected for mass variation, average drug contents

Table 2
Drug contents of pieces of HPC-based filament with 48 % mannitol (2 batches, n = 3 per batch, mean ± SD).

Filament batch	Weight (mg)	Total drug content (mg)	Total drug content (w/w%)	Average content (w/w %)
1	520.3	21.1	4.06	4.07 ± 0.09
	673.8	26.7	3.97	
	642.4	26.9	4.19	
2	679.4	30.0	4.42	4.45 ± 0.02
	954.9	42.6	4.46	
	974.8	43.6	4.47	

expressed in percentages showed that content uniformity was high within batches but low between batches. Suppository A (no mannitol) had a drug content of 3.26 ± 0.31 w/w% and suppository B (23 % mannitol) had a drug content of 3.76 ± 0.30 w/w%, as both were printed from different batches. Suppositories C, D, and E (48 % mannitol) were printed with another filament batch and had similar drug contents when compared to each other. Suppositories F and G (48 % mannitol) were printed from another batch and also had drug contents that differed from other batches but were similar when compared to each other. These results can be explained by the drug content variations in filaments as discussed in section 3.3.1.

Compared to Domsta et al. (2022) who printed suppositories by SSE, drug content uniformity in our study was low. However, when compared to FDM printing of oral medication, drug content uniformities were found similar to our results. According to the systematic review of Brambilla et al. (2021), in 57 % of FDM articles uniformity of weight is tested, and in 68 % of FDM articles drug content is analyzed (n = 69). Differences in drug content were either attributed to stickiness of the drug during the manufacturing process or to degradation due to high temperatures (Genina et al., 2017; Goyanes et al., 2015a). Our study affirms that further improvement to the FDM printing technique is needed and that careful selection of candidate drugs is necessary for FDM printing.

Furthermore, the results in Table 3 show that the drug content within a batch was less variable when mannitol was added. A possible explanation for this observation is that the flowability of the powders during extrusion is improved upon addition of mannitol, thus improving the homogeneity of the powders in the extruder formulation. The Hausner ratios of the formulations as calculated from their bulk density and tapped density confirmed this hypothesis. (Table S3).

UPLC analyses of printed objects showed peaks of the prednisolone base, indicating that ester hydrolysis took place (Fig. S2). For instance, the average PSP content of suppository C was 15.99 ± 0.81 mg, whereas the average amount of PSP converted to prednisolone base was 2.23 ± 0.52 mg (n = 3, Table S3). The average hydrolysis of all analyzed suppositories with 48 % mannitol (C–G in triplicate) was 11.3 ± 5.3 % (n = 15), compared to an average of only 1.7 ± 1.2 % for the analyzed filaments with 48 % mannitol (n = 6). Since more hydrolysis took place in suppositories than in filaments, and no further hydrolysis was observed in the dissolution medium after complete release of the drug, a large proportion of this hydrolysis is likely caused by the higher temperature of the printing process (Fig. S2 and S3). Therefore, hydrolysis could likely be reduced by decreasing the printing temperature. Alternatively, corticosteroids with higher thermostability could be used in this formulation.

From a pharmacological view, a small fraction of the drug being converted to prednisolone base is not problematic as PSP is a water-soluble prodrug that is rapidly dephosphorylated in the gastrointestinal tract to the more hydrophobic prednisolone which subsequently can be absorbed over the epithelial wall (Smits et al., 2015). However, from a biopharmaceutical view, conversion could theoretically cause solubility issues. In addition to the prednisolone base, two other unidentified peaks with very small areas were observed, but these were also present in the raw PSP and thus not a consequence of extrusion or printing (Fig. S4).

Furthermore, during the HME process, the materials are subjected to physical forces, such as friction and shear stress, that could potentially accelerate degradation even at extrusion temperatures lower than the degradation temperature of some drugs. In addition to examination of thermal sensitivity, resistance of the drug to physical stress should therefore be assessed thoroughly before manufacturing pharmaceuticals using extrusion techniques.

Since the addition of mannitol seemed to improve the consistency of filament diameter, this consequently seemed to improve the reproducibility of prints, especially within batches (Table 3). This explains the lower absolute and relative mass variation of suppositories C, D, and E compared to suppositories A and B. Relative mass variation was higher for suppositories F and G than for A and B. However, absolute mass variation was lower for F and G, indicating that relative mass variation was only higher due to the lower masses of the smaller suppositories.

Reducing the variation between batches would improve overall reproducibility. Since the programmed print speed in mm/s and the flow of the 3D-printing process were constant, variations in filament diameters would cause variations in the quantity of material printed. Therefore, filament diameter variation is likely the main reason for the mass variation of the printed suppositories. In practice, this problem could be overcome without changing the printer specifications when filament production processes are more standardized. Alternatively, one could design printhead setups in which the deposition speed of the filament is less depending on the feeding rate of the filament which most likely also results in longer contact times of the formulation with the heated print head. Since this is not desirable, a more diligent production of standardized filaments seems preferable.

Fig. 3 shows the correlation between mass and drug content of all printed suppositories containing 48 % mannitol. Linear regression showed that the coefficient of determination is > 0.99, and all data points were within the 99 % confidence interval, indicating a strong correlation between mass and drug content. Variation between suppositories is therefore mainly caused by variation in mass, and not by variation in drug content. The correlation does not intercept the origin because the variation between batches affects the slope of the curve. As expected, when both batches are plotted separately, their interceptions are closer to zero. These results demonstrate that adjustment of printed mass is an appropriate method for dose tuning. Furthermore, they prove that filament quality is decisive for reproducibility. Consistent reproducibility of 3D-printed medicine can be accomplished by future improvement of HME technology.

Table 3
Mass and drug content of 3D-printed suppositories (n = 3, mean ± SD).

Suppository	Infill density (%)	Height (mm)	Average mass (mg)	Average drug content (mg)	Average drug content (w/w%)	Percentage of theoretical load (%)
A	20	26	652.2 ± 49.5	21.4 ± 3.3	3.26 ± 0.31	81.50 ± 7.75
B	20	26	701.4 ± 54.1	26.5 ± 3.7	3.76 ± 0.30	94.00 ± 7.50
C	20	26	587.2 ± 8.8	18.2 ± 0.3	3.10 ± 0.02	77.50 ± 0.50
D	50	26	734.5 ± 24.7	22.2 ± 1.2	3.03 ± 0.07	75.75 ± 1.75
E	80	26	961.0 ± 10.4	30.0 ± 0.2	3.13 ± 0.02	78.25 ± 0.50
F	20	21	343.4 ± 28.9	8.9 ± 0.8	2.58 ± 0.03	64.50 ± 0.75
G	20	16	242.5 ± 22.2	6.3 ± 0.6	2.60 ± 0.03	65.00 ± 0.75

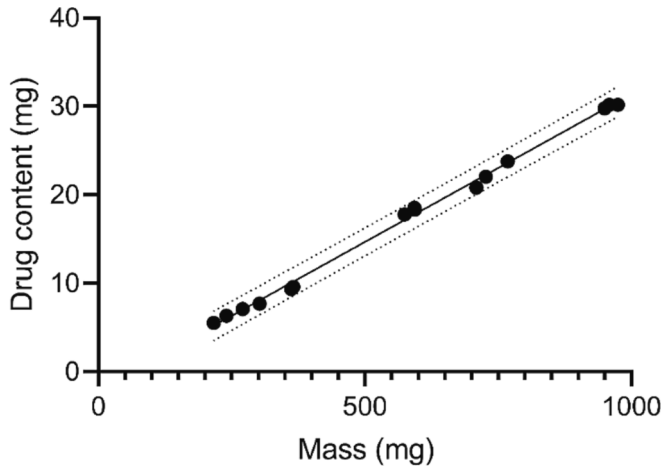

Fig. 3. Correlation between mass and drug content of suppositories containing 48% mannitol (suppositories C, D, E, F, and G). The dotted lines indicate the 99% confidence interval.

3.3.3. *Imaging of filaments and suppositories*

Filaments and suppositories showed a slightly yellowish color (Fig. 4). It is unlikely that this was caused by degradation of PSP but rather due to colorization of HPC, since potential degradation was investigated (see section 3.3.2). Furthermore, colorization also occurred in filaments and suppositories without drug.

SEM images of cross sections of filaments and suppositories without mannitol showed that PSP is distributed throughout the amorphous HPC matrix as crystalline material (Fig. 4a and 4b). In the filaments and suppositories with mannitol added, mannitol crystals could be seen distributed homogeneously throughout the matrix (Fig. 4c, 4d, 4e, and 4f). In these images, no distinction between drug and mannitol crystals could be made. However, the presence of mannitol crystals was certain because of the large quantity of crystals observed. SEM images of filaments showed rough surfaces because they were broken prior to imaging, whereas SEM images of suppositories show flat surfaces due to breaking off smoothly between printed layers.

3.3.4. *Thermal and morphological studies of formulations*

DSC analysis of the powder mixture, filament, and suppository with 4 % PSP and 48 % mannitol showed similar thermograms for all materials, demonstrating that the endothermic peak of mannitol was still visible after HME and 3D-printing (Fig. 5a). Since HME and 3D-printing were performed below the melting temperature of mannitol (at 130 °C and 150 °C respectively), no melting occurred and mannitol expectedly remained crystalline. This is also supported by the crystalline patterns of mannitol that can be observed in the PXRD results of the filament and suppository (Fig. 5b).

Although the SEM images in Fig. 4 confirmed the presence of crystalline PSP, quantification of potential amorphization of a fraction of PSP was not possible with DSC (no peaks discernable in the raw material

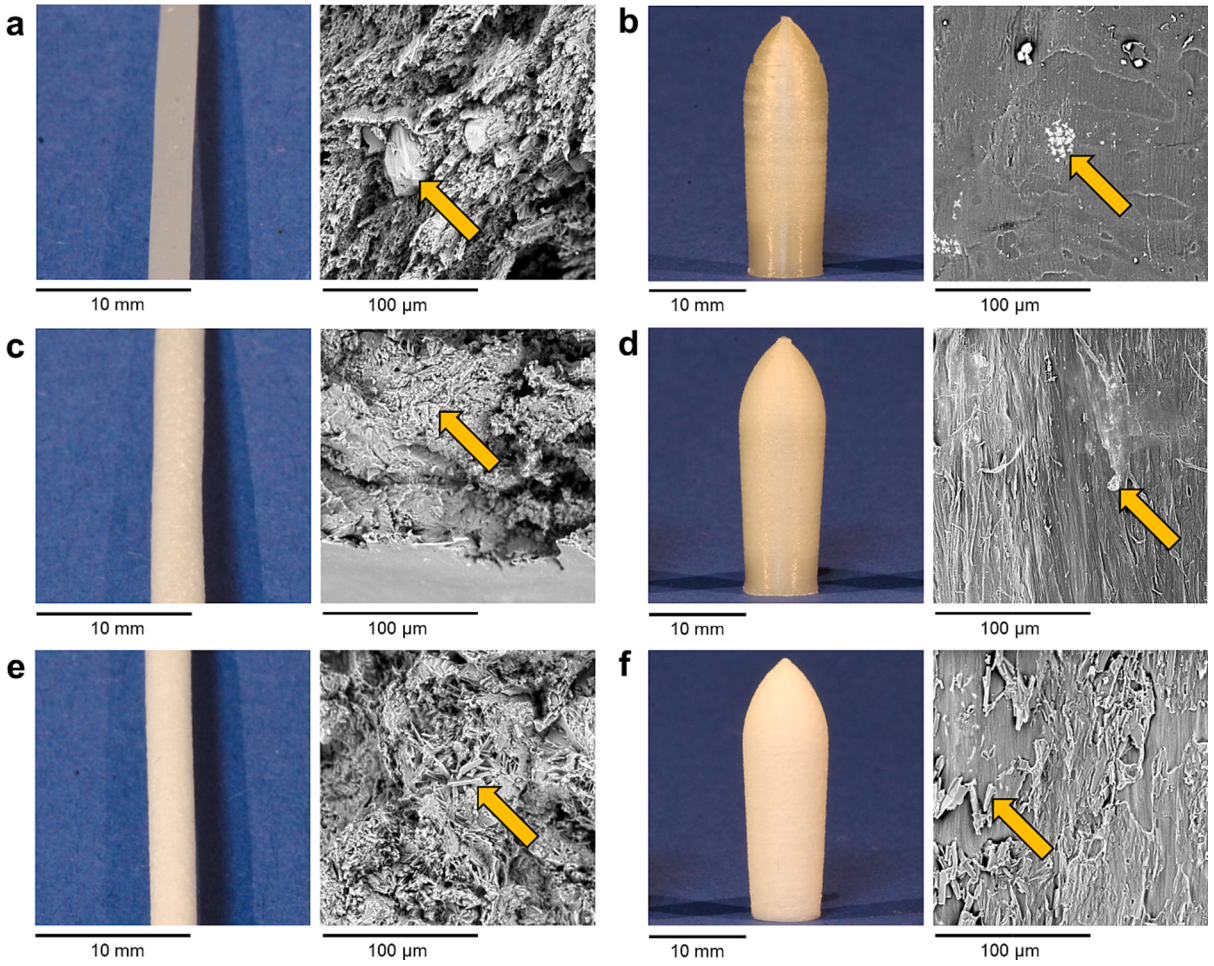

Fig. 4. Photographs of drug-loaded filaments and suppositories and scanning electron micrographs of their cross sections with a magnification of 1500x. Yellow arrows indicate crystalline material. a) Filament without mannitol. b) Suppository without mannitol. c) Filament with 23% mannitol. d) Suppository with 23% mannitol. e) Filament with 48% mannitol. f) Suppository with 48% mannitol.

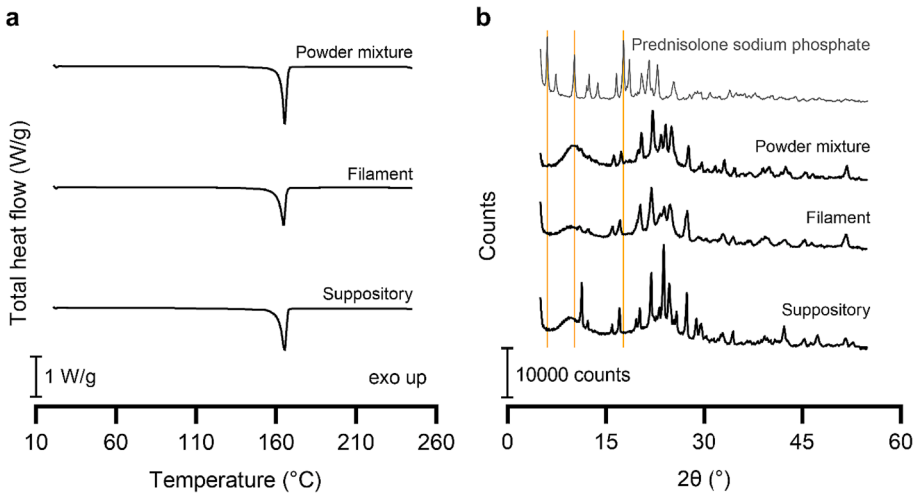

Fig. 5. Physico-chemical characterization of the formulation with 48% mannitol. a) Differential scanning calorimetry of the powder mixture, filament, and suppository. b) Powder X-ray diffraction of the powder mixture, filament, and suppository. The pattern of prednisolone sodium phosphate is shown again and the vertical yellow lines indicate the absence of its characteristic peaks in the formulation.

as shown in Fig. 2a or in the powder mixture as shown in Fig. 5a) or PXRD (no characteristic PSP peaks detectable in the powder mixture, see Fig. 5b). Although it is possible that PSP is partially amorphized during extrusion and 3D-printing, analytical quantification by PXRD is limited due to the low concentration of PSP.

3.4. Dissolution tests of suppositories

3.4.1. Effect of mannitol concentration on drug release of suppositories

We performed dissolution tests to investigate the effect of mannitol in the formulation on the drug release rate. The dissolution experiments demonstrated that the drug release rate from the suppositories increases with a higher concentration of mannitol (Fig. 6c). The suppository with the highest concentration of mannitol (48 %) showed the highest drug release rate, releasing 90 % of the PSP within 30 min. The suppository with 23 % mannitol showed a slightly increased drug release rate compared to the suppository without mannitol. The latter released less than 25 % of the PSP after 30 min and approximately 75 % of the PSP after 120 min. Thus, we achieved rapid release by adding 48 % mannitol to the formulation as a pore former.

Interestingly, the release rate of the suppository with 48 % mannitol was remarkably higher than the release rate of the suppository with 23 % mannitol. Hence, we hypothesize that the percolation threshold for mannitol is reached between a concentration of 23 % and 48 %. The percolation threshold is the concentration at which the particles of a component form an infinite cluster through the whole matrix (Caraballo, 2010). It is likely that the increased release rate can be explained by an improved influx of water into the core of the suppositories accelerating dissolution of the drug, as well as enhanced diffusion and release of PSP via these pores before gelation of the dosage form. A faster dissolution of the matrix was visually observed in the dissolution studies.

The results show that our formulations could be employed for both rapid release, i.e., by employing high mannitol content, as well as for sustained release when less or no mannitol is added into the suppository's matrix.

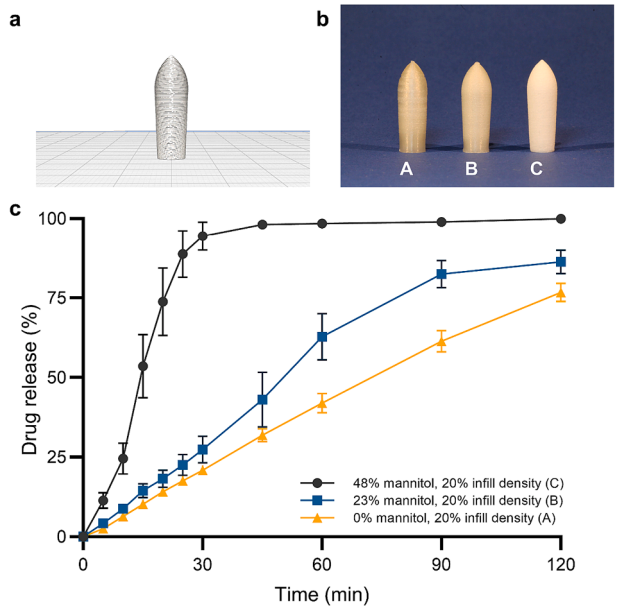

Fig. 6. a) Sliced suppository CAD models. b) Photograph of 3D-printed suppositories with different concentrations of mannitol. c) Dissolution profiles of suppositories with different concentrations of mannitol.

3.4.2. Effects of suppository infill density and dimensions on dose and release rate

Using the filaments with 48 % mannitol, suppositories with various infill densities (20, 50, and 80 %) and dimensions (16, 21, and 26 mm in height) were printed. The weight of the suppositories, and therefore the dosage of PSP, increased by printing with a higher infill density and, alternatively, decreased by printing smaller suppositories (Table 3). We followed both approaches, which provides a wide theoretical dose range for our printed suppositories from 6 mg (smallest dimension with lowest infill density) to 30 mg (largest dimension with highest infill density), thus covering patient characteristics corresponding to 6 kg body weight and 30 kg body weight (dose advise 1 mg/kg until 18 years of age). Previous studies only investigated how dose ranges of printed dosage units can be varied by changing their dimensions (Pietrzak et al., 2015; Gorkem et al., 2020). However, changing the dimensions could negatively affect patient acceptability (Goyanes et al., 2017). This can be avoided by utilizing the infill density rather than changing the dimensions. Conversely, smaller dimensions of suppositories can potentially increase patient acceptability.

Many studies have utilized the infill density to modify release profiles (Solanki et al., 2018; Korte and Quodbach, 2018b; Thakkar et al., 2020). This effect is unintended if the purpose is to tune the dosage. We hypothesize that the influence of the infill density on the release rate can be diminished greatly through the addition of mannitol in our study.

Therefore, dissolution tests for 3D-printed suppositories with different infill densities were performed to assess whether the drug release remains within an acceptable range (Fig. 7c).

As expected, the dissolution results in Fig. 7c showed that the release rate was not notably affected by the infill density between 20 % and 50 %. We demonstrated dose-independent drug release between 18 and 22 mg by adding mannitol to this formulation. However, with an infill density of 80 %, the drug release rate decreased, demonstrating that there is a limit to tuning the dose by varying infill densities. Nevertheless, the release rate of the suppository with 80 % infill density was still higher than the formulations with 0 % or 23 % mannitol as shown in Fig. 6. In another study, dose-independent drug release of 3D-printed medicines with variable dosages was achieved by keeping the surface-area-to-volume ratio alike (Windolf et al., 2022). It is essential to assess whether changes in drug release profiles are within acceptable limits before changing the infill density to tune the dose.

After demonstrating that the dose can be tuned by varying infill density, we examined the possibility of tuning the dose by printing suppositories with smaller dimensions. The dissolution data showed that smaller suppositories are associated with lower doses of PSP, while the relative release of the drug stays similar (Fig. 8c). All standard suppositories including suppository C were 26 mm in height, based on 1.15 ml suppository molds used for infants. Both the small suppository F (21 mm in height) and the extra small suppository G (16 mm in height) contained dosages suitable for infants (approximately 9 mg and 6 mg, respectively), and will presumably have higher acceptability by infants because of their reduced dimensions.

Previous research has shown that dissolution rates are faster for smaller 3D-printed pharmaceuticals due to their higher surface-area-to-volume ratio (Goyanes et al., 2015b). However, this relation is not observed in our suppositories, most likely because of the rapid drug release caused by the addition of a pore former.

Dosages could be adjusted even further by changing the infill density of small and extra small suppositories as well, or by further changing the size, thus proving the versatility of 3D-printing for dose tuning and adjustment of release profile.

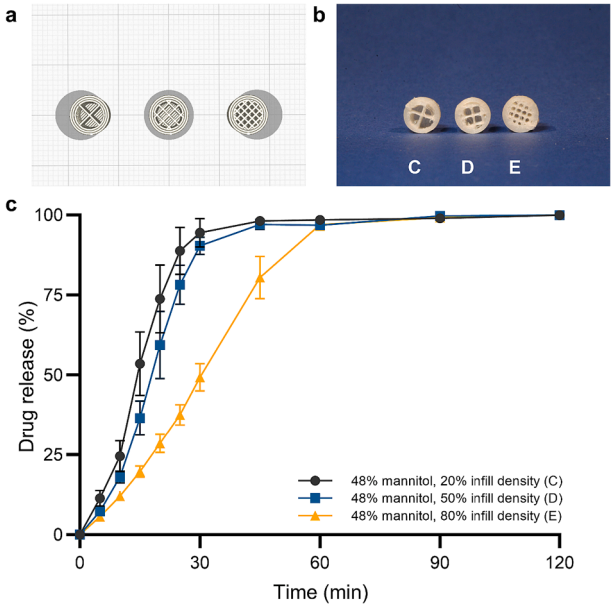

Fig. 7. a) Cross sections of sliced suppository CAD models with different infill densities. b) Photograph of cross sections of 3D-printed suppositories with different infill densities. c) Dissolution profiles of suppositories with different infill densities.

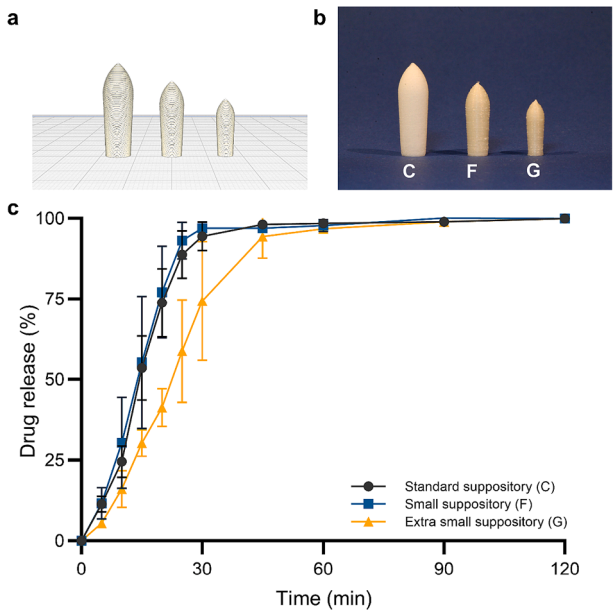

Fig. 8. a) Sliced suppository CAD models with different dimensions. b) Photograph of 3D-printed suppositories with different dimensions. c) Dissolution profiles of suppositories with different dimensions.

4. Conclusions

We have successfully designed and 3D-printed prednisolone phosphate-loaded suppositories with tunable dose and rapid drug release. The addition of mannitol as a pore-forming excipient to the formulation greatly increased the dissolution rate. Furthermore, due to the fast dissolution of the preparation, altering the infill density or dimensions of the suppositories to change the dose did not notably affect the release profiles of prednisolone. Therefore, it can be expected that 3D-printed prednisolone suppositories with different doses will have similar pharmacokinetics when administered to IBD patients, and hence similar therapeutic efficacies. Thus, 3D-printing proves to be a useful technology to develop precision medicine and meet the needs of individual patients, not only by making adjustments of the dose to the body weight of a patient possible but also by enabling the production of novel dosage forms in a variety of shapes and dimensions. Furthermore, this flexibility is easily accomplished by altering digital print settings without having to change the formulation. This will automate the preparation of custom formulations by manufacturers and compounding pharmacies, especially if filament production is standardized. As a result, 3D-printing is a promising technology to improve the outcome of medical treatments. Future studies regarding the suitability and safety of various polymers for the rectal administration route, the prevention of ester hydrolysis, and the improvement of reproducibility by achieving higher content uniformity with enhanced extrusion technology will contribute to expanding the many pharmaceutical applications of 3D-printing.

Funding.

This research did not receive any specific grant from funding agencies in the public, commercial, or not-for-profit sectors.

CRediT authorship contribution statement

L.I. Kocabas: Conceptualization, Methodology, Investigation, Data curation, Writing – original draft, Visualization, Project administration. **S. Ayyoubi:** . **M. Tajqurishi:** . **J. Quodbach:** Writing – review & editing, Supervision. **T. Vermonden:** . **R.J. Kok:** Writing – review & editing, Supervision, Funding acquisition.

Declaration of competing interest

The authors declare that they have no known competing financial interests or personal relationships that could have appeared to influence the work reported in this paper.

Data availability

Data will be made available on request.

Acknowledgments

The authors would like to thank T. Lashkari who provided technical assistance for scanning electron microscopy, M.J. van Steenbergen who provided technical assistance for thermogravimetric analysis and differential scanning calorimetry, and D.F.L. Wezendonk who provided technical assistance for powder X-ray diffraction.

Appendix A. Supplementary data

Supplementary data to this article can be found online at https://doi.org/10.1016/j.ijpharm.2023.123639.

References

Arenas-López, S., Gurung, K., Tibby, S.M., Calleja Hernández, M.Á., Tuleu, C., 2017. Accuracy of enteral syringes with commonly prescribed paediatric liquid medicines. Arch. Dis. Child. 102 (7), 659. https://doi.org/10.1136/archdischild-2016-312492.

Awad, A., Hollis, E., Goyanes, A., Orlu, M., Gaisford, S., Basit, A.W., 2023a. 3D printed multi-drug-loaded suppositories for acute severe ulcerative colitis. International Journal of Pharmaceutics: X 5, 100165. https://doi.org/10.1016/j.ijpx.2023.100165.

Awad, A., Goyanes, A., Orlu, M., Gaisford, S., Basit, A.W., 2023b. 3D printed infliximab suppositories for rectal biologic delivery. International Journal of Pharmaceutics: X 5, 100176. https://doi.org/10.1016/j.ijpx.2023.100176.

Berthold, A., Cremer, K., Kreuter, J., 1996. Preparation and characterization of chitosan microspheres as drug carrier for prednisolone sodium phosphate as model for anti-inflammatory drugs. J. Control. Release 39 (1), 17–25. https://doi.org/10.1016/0168-3659(95)00129-8.

Bowles, A., Keane, J., Ernest, T., Clapham, D., Tuleu, C., 2010. Specific aspects of gastrointestinal transit in children for drug delivery design. Int. J. Pharm. 395 (1), 37–43. https://doi.org/10.1016/j.ijpharm.2010.04.048.

Brambilla, C.R.M., Okafor-Muo, O.L., Hassanin, H., ElShaer, A., 2021. 3DP Printing of Oral Solid Formulations: A Systematic Review. Pharmaceutics 13 (3), 358. https://doi.org/10.3390/pharmaceutics13030358.

Cailleaux, S., Sanchez-Ballester, N.M., Gueche, Y.A., Bataille, B., Soulairol, I., 2021. Fused Deposition Modeling (FDM), the new asset for the production of tailored medicines. J. Control. Release 330, 821–841. https://doi.org/10.1016/j.jconrel.2020.10.056.

Caraballo, I., 2010. Factors affecting drug release from hydroxypropyl methylcellulose matrix systems in the light of classical and percolation theories. Expert Opin. Drug Deliv. 7 (11), 1291–1301. https://doi.org/10.1517/17425247.2010.528199.

Chatzitaki, A., Tsongas, K., Tzimtzimis, E.K., Tzetzis, D., Bouropoulos, N., Barmpalexis, P., Eleftheriadis, G.K., Fatouros, D.G., 2021. 3D printing of patient-tailored SNEDDS-based suppositories of lidocaine. J. Drug Delivery Sci. Technol. 61, 102292 https://doi.org/10.1016/j.jddst.2020.102292.

Choi, H., Jung, J., Ryu, J., Yoon, S., Oh, Y., Kim, C., 1998. Development of in situ-gelling and mucoadhesive acetaminophen liquid suppository. Int. J. Pharm. 165 (1), 33–44. https://doi.org/10.1016/S0378-5173(97)00386-4.

Domsta, V., Krause, J., Weitschies, W., Seidlitz, A., 2022. 3D Printing of Paracetamol Suppositories: An Automated Manufacturing Technique for Individualized Therapy. Pharmaceutics 14 (12), 2676. https://doi.org/10.3390/pharmaceutics14122676.

Dumpa, N., Butreddy, A., Wang, H., Komanduri, N., Bandari, S., Repka, M.A., 2021. 3D printing in personalized drug delivery: An overview of hot-melt extrusion-based fused deposition modeling. Int. J. Pharm. 600, 120501 https://doi.org/10.1016/j.ijpharm.2021.120501.

Elliott, J.P., McConaha, J., Cornish, N., Bunk, E., Hilton, L., Modany, A., Bucker, I., 2014. Influence of Viscosity and Consumer Use on Accuracy of Oral Medication Dosing Devices. J. Pharm. Technol. 30 (4), 111–117. https://doi.org/10.1177/8755122514533780.

Fan, D., Li, Y., Wang, X., Zhu, T., Wang, Q., Cai, H., Li, W., Tian, Y., Liu, Z., 2020. Progressive 3D Printing Technology and Its Application in Medical Materials. Front. Pharmacol. 11, 122. https://doi.org/10.3389/fphar.2020.00122.

Fanous, M., Gold, S., Hirsch, S., Ogorka, J., Imanidis, G., 2020. Development of immediate release (IR) 3D-printed oral dosage forms with focus on industrial relevance. Eur. J. Pharm. Sci. 155, 105558 https://doi.org/10.1016/j.ejps.2020.105558.

Genina, N., Boetker, J.P., Colombo, S., Harmankaya, N., Rantanen, J., Bohr, A., 2017. Anti-tuberculosis drug combination for controlled oral delivery using 3D printed compartmental dosage forms: From drug product design to in vivo testing. J. Control. Release 268, 40–48. https://doi.org/10.1016/j.jconrel.2017.10.003.

Gorkem Buyukgoz, G., Soffer, D., Defendre, J., Pizzano, G.M., Davé, R.N., 2020. Exploring tablet design options for tailoring drug release and dose via fused deposition modeling (FDM) 3D printing. Int. J. Pharm. 591, 119987 https://doi.org/10.1016/j.ijpharm.2020.119987.

Goyanes, A., Buanz, A.B.M., Hatton, G.B., Gaisford, S., Basit, A.W., 2015a. 3D printing of modified-release aminosalicylate (4-ASA and 5-ASA) tablets. Eur. J. Pharm. Biopharm. 89, 157–162. https://doi.org/10.1016/j.ejpb.2014.12.003.

Goyanes, A., Robles Martinez, P., Buanz, A., Basit, A.W., Gaisford, S., 2015b. Effect of geometry on drug release from 3D printed tablets. Int. J. Pharm. 494 (2), 657–663. https://doi.org/10.1016/j.ijpharm.2015.04.069.

Goyanes, A., Fina, F., Martorana, A., Sedough, D., Gaisford, S., Basit, A.W., 2017a. Development of modified release 3D printed tablets (printlets) with pharmaceutical excipients using additive manufacturing. Int. J. Pharm. 527 (1–2), 21–30. https://doi.org/10.1016/j.ijpharm.2017.05.021.

Goyanes, A., Scarpa, M., Kamlow, M., Gaisford, S., Basit, A.W., Orlu, M., 2017b. Patient acceptability of 3D printed medicines. Int. J. Pharm. 530 (1–2), 71–78. https://doi.org/10.1016/j.ijpharm.2017.07.064.

Ashland Inc. (2017). *Klucel™ hydroxypropylcellulose - Physical and chemical properties*. https://www.ashland.com/file_source/Ashland/Product/Documents/Pharmaceutical/PC_11229_Klucel_HPC.pdf.

Jaipal, A., Pandey, M.M., Charde, S.Y., Raut, P.P., Prasanth, K.V., Prasad, R.G., 2015. Effect of HPMC and mannitol on drug release and bioadhesion behavior of buccal discs of buspirone hydrochloride: In-vitro and in-vivo pharmacokinetic studies. Saudi Pharmaceutical Journal 23 (3), 315–326. https://doi.org/10.1016/j.jsps.2014.11.012.

Jannin, V., Lemagnen, G., Gueroult, P., Larrouture, D., Tuleu, C., 2014. Rectal route in the 21st Century to treat children. Adv. Drug Deliv. Rev. 73, 34–49. https://doi.org/10.1016/j.addr.2014.05.012.

Jeong, D.Y., Kim, S., Son, M.J., Son, C.Y., Kim, J.Y., Kronbichler, A., Lee, K.H., Shin, J.I., 2019. Induction and maintenance treatment of inflammatory bowel disease: A comprehensive review. Autoimmun. Rev. 18 (5), 439–454. https://doi.org/10.1016/j.autrev.2019.03.002.

Karavasili, C., Gkaragkounis, A., Fatouros, D.G., 2021. Patent landscape of pediatric-friendly oral dosage forms and administration devices. Expert Opin. Ther. Pat. 31 (7), 663–685. https://doi.org/10.1080/13543776.2021.1893691.

Kelsen, J.R., Russo, P., Sullivan, K.E., 2019. Early-Onset Inflammatory Bowel Disease. Immunol. Allergy Clin. North Am. 39 (1), 63–79. https://doi.org/10.1016/j.iac.2018.08.008.

Kim, S., Chen, J., Cheng, T., Gindulyte, A., He, J., He, S., Li, Q., Shoemaker, B.A., Thiessen, P.A., Yu, B., Zaslavsky, L., Zhang, J., Bolton, E.E., 2023. PubChem 2023 update. Nucleic Acids Res. 51 (D1), D1373–D1380. https://doi.org/10.1093/nar/gkac956.

Korte, C., Quodbach, J., 2018a. 3D-printed network structures as controlled-release drug delivery systems: Dose adjustment, API release analysis and prediction. AAPS PharmSciTech 19 (8), 3333–3342. https://doi.org/10.1208/s12249-018-1017-0.

Korte, C., Quodbach, J., 2018b. Formulation development and process analysis of drug-loaded filaments manufactured via hot-melt extrusion for 3D-printing of medicines. Pharm. Dev. Technol. 23 (10), 1117–1127. https://doi.org/10.1080/10837450.2018.1433208.

Krezić, S., Krhan, E., Mandžuka, E., Kovač, N., Krajina, D., Marić, A., Komić, S., Nikšić, A., Tucak, A., Sirbubalo, M., Vranić, E., 2019. Fabrication of rectal and vaginal suppositories using 3D printed moulds: The challenge of personalized therapy. In: CMBEBIH 2019. Springer International Publishing AG, pp. 729–734.

Marshall, J.K., Irvine, E.J., 1997. Rectal corticosteroids versus alternative treatments in ulcerative colitis: a meta-analysis. Gut 40 (6), 775–781. https://doi.org/10.1136/gut.40.6.775.

Patil, H., Tiwari, R.V., Repka, M.A., 2016. Hot-melt extrusion: from Theory to application in pharmaceutical formulation. AAPS PharmSciTech 17 (1), 20–42. https://doi.org/10.1208/s12249-015-0360-7.

Persaud, S., Eid, S., Swiderski, N., Serris, I., Cho, H., 2020. Preparations of rectal suppositories containing artesunate. Pharmaceutics 12 (3), 222. https://doi.org/10.3390/pharmaceutics12030222.

Pietrzak, K., Isreb, A., Alhnan, M.A., 2015. A flexible-dose dispenser for immediate and extended release 3D printed tablets. Eur. J. Pharm. Biopharm. 96, 380–387. https://doi.org/10.1016/j.ejpb.2015.07.027.

Ponsar, H., Wiedey, R., Quodbach, J., 2020. Hot-melt extrusion process fluctuations and their impact on critical quality attributes of filaments and 3d-printed dosage forms. Pharmaceutics 12 (6), 511. https://doi.org/10.3390/pharmaceutics12060511.

Purohit, T.J., Hanning, S.M., Wu, Z., 2018. Advances in rectal drug delivery systems. Pharm. Dev. Technol. 23 (10), 942–952. https://doi.org/10.1080/10837450.2018.1484766.

Rathi, R., Sanshita, Kumar, A., Vishvakarma, V., Huanbutta, K., Singh, I., & Sangnim, T. (2022). Advancements in Rectal Drug Delivery Systems: Clinical Trials, and Patents Perspective. *Pharmaceutics, 14*(10), 2210. doi: 10.3390/pharmaceutics14102210.

Robles-Martinez, P., Xu, X., Trenfield, S.J., Awad, A., Goyanes, A., Telford, R., Basit, A.W., Gaisford, S., 2019. 3D Printing of a multi-layered polypill containing six drugs using a novel stereolithographic method. Pharmaceutics 11 (6), 274. https://doi.org/10.3390/pharmaceutics11060274.

Rosen, M.J., Dhawan, A., Saeed, S.A., 2015. Inflammatory bowel disease in children and adolescents. JAMA Pediatr. 169 (11), 1–8. https://doi.org/10.1001/jamapediatrics.2015.1982.

Ryu, J., Chung, S., Lee, M., Kim, C., Shim, C.-K., 1999. Increased bioavailability of propranolol in rats by retaining thermally gelling liquid suppositories in the rectum. J. Control. Release 59 (2), 163–172. https://doi.org/10.1016/S0168-3659(98)00189-8.

Sadia, M., Sośnicka, A., Arafat, B., Isreb, A., Ahmed, W., Kelarakis, A., Alhnan, M.A., 2016. Adaptation of pharmaceutical excipients to FDM 3D printing for the fabrication of patient-tailored immediate release tablets. Int. J. Pharm. 513 (1–2), 659–668. https://doi.org/10.1016/j.ijpharm.2016.09.050.

Seoane-Viaño, I., Ong, J.J., Luzardo-Álvarez, A., González-Barcia, M., Basit, A.W., Otero-Espinar, F.J., Goyanes, A., 2021. 3D printed tacrolimus suppositories for the treatment of ulcerative colitis. Asian Journal of Pharmceutical Sciences 16 (1), 110–119. https://doi.org/10.1016/j.ajps.2020.06.003.

Simões, M.F., Pinto, R.M.A., Simões, S., 2021. Hot-melt extrusion: A roadmap for product development. AAPS PharmSciTech 22 (5), 184. https://doi.org/10.1208/s12249-021-02017-7.

Sjöholm, E., Mathiyalagan, R., Rajan Prakash, D., Lindfors, L., Wang, Q., Wang, X., Ojala, S., Sandler, N., 2020. 3D-printed veterinary dosage forms—a comparative study of three semi-solid extrusion 3D printers. Pharmaceutics 12 (12), 1239. https://doi.org/10.3390/pharmaceutics12121239.

Skowyra, J., Pietrzak, K., Alhnan, M.A., 2015. Fabrication of extended-release patient-tailored prednisolone tablets via fused deposition modelling (FDM) 3D printing. Eur. J. Pharm. Sci. 68, 11–17. https://doi.org/10.1016/j.ejps.2014.11.009.

Smits, E.A.W., Soetekouw, J.A., van Doormalen, I., van den Berg, B.H.J., van der Woude, M.P., de Wijs-Rot, N., Vromans, H., 2015. Quantitative LC–MS determination of liposomal encapsulated prednisolone phosphate and non-encapsulated prednisolone concentrations in murine whole blood and liver tissue. J. Pharm. Biomed. Anal. 115, 552–561. https://doi.org/10.1016/j.jpba.2015.07.012.

Sobhani, P., Christopherson, J., Ambrose, P.J., Corelli, R.L., 2008. Accuracy of oral liquid measuring devices: comparison of dosing cup and oral dosing syringe. Ann. Pharmacother. 42 (1), 46–52. https://doi.org/10.1345/aph.1K420.

Solanki, N.G., Tahsin, M., Shah, A.V., Serajuddin, A.T.M., 2018. Formulation of 3D printed tablet for rapid drug release by fused deposition modeling: Screening polymers for drug release, drug-polymer miscibility and printability. J. Pharm. Sci. 107 (1), 390–401. https://doi.org/10.1016/j.xphs.2017.10.021.

Tagami, T., Hayashi, N., Sakai, N., Ozeki, T., 2019. 3D printing of unique water-soluble polymer-based suppository shell for controlled drug release. Int. J. Pharm. 568, 118494 https://doi.org/10.1016/j.ijpharm.2019.118494.

Tagami, T., Ito, E., Hayashi, N., Sakai, N., Ozeki, T., 2020. Application of 3D printing technology for generating hollow-type suppository shells. Int. J. Pharm. 589, 119825 https://doi.org/10.1016/j.ijpharm.2020.119825.

Tenci, M., Rossi, S., Giannino, V., Vigani, B., Sandri, G., Bonferoni, M.C., Daglia, M., Longo, L.M., Macelloni, C., Ferrari, F., 2019. An in situ gelling system for the local treatment of inflammatory bowel disease (IBD). The loading of maqui (Aristotelia Chilensis). Berry Extract as an Antioxidant and Anti-Inflammatory Agent. *Pharmaceutics* 11 (11), 611. https://doi.org/10.3390/pharmaceutics11110611.

Thakkar, R., Pillai, A.R., Zhang, J., Zhang, Y., Kulkarni, V., Maniruzzaman, M., 2020. Novel on-demand 3-dimensional (3-D) printed tablets using fill density as an effective release-controlling tool. Polymers 12 (9), 1872. https://doi.org/10.3390/polym12091872.

Trenfield, S.J., Madla, C.M., Basit, A.W., Gaisford, S., 2018. The shape of things to come: Emerging applications of 3D printing in healthcare. In: 3D Printing of Pharmaceuticals. Springer International Publishing, pp. 1–19.

van Rheenen, P.F., Aloi, M., Assa, A., Bronsky, J., Escher, J.C., Fagerberg, U.L., Gasparetto, M., Gerasimidis, K., Griffiths, A., Henderson, P., Koletzko, S., Kolho, K., Levine, A., van Limbergen, J., Martin de Carpi, F.J., Navas-López, V.c.M., Oliva, S., de Ridder, L., Russell, R.K., Ruemmele, F.M., 2021. The medical management of paediatric crohn's disease: An ECCO-ESPGHAN guideline update. *J. Crohns Colitis* 15 (2), 171–194. https://doi.org/10.1093/ecco-jcc/jjaa161.

Windolf, H., Chamberlain, R., Quodbach, J., 2022. Dose-independent drug release from 3D printed oral medicines for patient-specific dosing to improve therapy safety. Int. J. Pharm. 616, 121555 https://doi.org/10.1016/j.ijpharm.2022.121555.